Ignazio Maria **Viola**[1] & Richard GJ **Flay**[2]

ON-WATER PRESSURE MEASUREMENTS ON A MODERN ASYMMETRIC SPINNAKER

Proceedings of the 21st International HISWA Symposium on Yacht Design and Yacht Construction, 15th-16th November 2010, Amsterdam, The Netherlands

Abstract

The present paper presents full-scale pressure measurements on sails set in downwind conditions. Pressure distributions were measured on a pressure-tapped asymmetric spinnaker. The sail was designed for Emirates Team New Zealand, a potential challenger for the 34th America's Cup, when it was expected to be sailed in AC33-class yachts. Pressure distributions were measured for several sail trims, and at three apparent wind angles, on both sides of the sail. Pressure distributions are discussed and correlated with the flow field. Full-scale pressure distributions are compared with wind-tunnel measurements. Good agreement and few differences were found.

1. Introduction

Sail aerodynamics has been widely investigated in the last century. Sails made from different materials and made in different shapes have been compared with on-water tests, wind tunnel tests and numerical codes. These three approaches allow different aspects of sail aerodynamics to be investigated. Unfortunately, each of them has some limitations, and none of them are able to substitute for the other two. The present paper investigates sail aerodynamics in downwind sailing conditions from on-water tests.

COMPUTATIONAL FLUID DYNAMICS

In the past few decades, numerical codes have become the most commonly used research tool for sails. In the 60s, potential-flow codes were used for 2D horizontal sail sections. In following years, the fast growth of computational resources led to Navier-Stokes codes being used more and more frequently. Nowadays, while potential-flow codes are widely used for upwind sailing conditions, Navier-Stokes codes are most commonly used for downwind conditions. In fact, in upwind conditions, sails are designed to operate near the maximum lift/drag ratio and, therefore, the flow has an attached boundary layer on most of the sail surface. Potential-flow codes, which are unable to model separated boundary layers, can compute aerodynamic forces with a reasonable accuracy in upwind conditions. Conversely, in downwind conditions, sails are designed to operate near the maximum lift and, therefore, they have more cambered sections and higher pressure gradients. The boundary layer separates before the trailing edge over a large part of the sail surface due to the high adverse pressure gradients. To correctly compute the aerodynamic forces, separation has to be computed correctly by modelling the viscosity of the fluid. Therefore, Navier-Stokes codes are commonly used to model downwind conditions.

Due to the relatively high sail Reynolds number, nowadays Direct Navier-Stokes simulations cannot be used in sail aerodynamics, even when very large computational resources are available (Viola & Ponzini, 2009). Therefore, Reynolds Averaged Navier-Stokes (RANS),

---

[1] Formerly Yacht Research Unit, The University of Auckland (New Zealand);
Since Sep. 2010, School of Marine Science and Technology, Newcastle University (UK).

[2] Yacht Research Unit, The University of Auckland (New Zealand);.

Large Eddy Simulations (LES) or Detached Eddy Simulations (DES) techniques have to be used to model the small-scale turbulence neglected by the limited grid resolution. These techniques use based on heuristic equations, which need to be validated with experimental measurements. Validations should be repeated every time the modelled geometry or the fluid characteristics are changed significantly. Therefore, wind-tunnel tests have to be performed for this purpose.

WIND TUNNEL TESTS

Wind tunnel tests allow the designer to have a real-time aerial view of the flying sails. Smoke visualization or other similar techniques allow streaklines to be visualised very efficiently. At the Yacht Research Unit, forces are measured with a 6-component balance located inside the boat model. It is common practice to use flexible sails, which can be trimmed remotely. Therefore, the change of forces and streaklines with change in the sail trim can be appreciated immediately. In most of the wind tunnels where sail aerodynamics is investigated, special devices allow the flying shapes to be detected. Thus the aerodynamic forces and flying shapes are recorded simultaneously. This increases the repeatability of the measurements and allows differences between sails and trims to be better appreciated. It also allows flying shapes to be modelled with numerical codes and computed forces to be compared with measured forces. However, validating numerical simulations just with forces is not ideal. In fact, the pressure distribution on sails might be computed incorrectly even when the computed resultant aerodynamic forces agreed with the measured force. This is because different pressure distributions can lead to the same global aerodynamic force. For this reason, in recent years, a great deal of effort has been put into measuring pressure distribution on sails with the aim of validating numerical codes (Viola & Flay, 2009; Viola et al, submitted).

Using flexible sails in wind tunnel tests allows different trims to be investigated. The deformation of the mast should be correctly modelled because it has a significant affect on the sail shape and on the sail position with respect of the longitudinal boat axis. Wind tunnel tests are usually performed at wind speeds between 2 m/s and 5 m/s. In wind tunnels with large test sections, the model-scale is of the order of 1/10 of full-scale. As a consequence, in order to achieve the full-scale Reynolds number, the wind tunnel wind speed should be 10 times higher than the full-scale wind speed. Unfortunately however, the maximum wind tunnel wind speed is usually equal to or less than the full-scale wind speed. This is because the flexible sails and rigging do not allow testing in high-speed conditions, as they would break!

The attitude of a sail flying high and far from the yacht depends on the ratio between the pressure distribution and the gravity force. Therefore, the weight of the model-scale sails should be chosen to achieve the same full-scale ratio between the pressures forces and the gravity force. This criterion leads to the choice of a very light model-scale sailcloth. However, since, the sail is a membrane, such a lightweight cloth would stretch a considerable amount due to the loads it be subjected to, and this change in shape would alter the aerodynamic loading. Unless the mast is especially bendy, where it needs to bend in the wind tunnel tests, the mast is usually modelled in its deformed “sailing” shape and, often, the sail is cut to its “flying” shape. Thus the wind tunnel tests the sails in the correct flying attitude, and thus properly simulates full-scale.

ON-WATER TESTS

Both numerical simulations and wind tunnel tests are simplified models of the complex full-scale conditions. When yachts sail, the dynamic movements of the yacht and of the sails are considerable. Moreover, the yacht sails through the turbulent atmospheric boundary layer, which leads to a time dependent flow pattern. The sails are continuously trimmed to take into account the dynamic movements of the yacht, the sails, and the change in the wind speed and direction. All these dynamic effects are modelled with difficulty (and consequently with low

accuracy) in CFD, and are normally not modelled in wind tunnel, except in special "dynamic" tests.

Because of the complexity of these dynamic effects, on-water tests are very difficult to perform and suffer from poor repeatability, thus leading to large uncertainty in the results. Firstly, the fully three-dimensional time dependent wind flow, in which the yacht sails, cannot be measured. For instance, if an anemometer were fixed on the top of the mast to measure the three wind velocity components, the measurement would be affected significantly by the influence of the sail trim. Moreover, even if the flow field was known at a location near the top of the mast, the apparent wind speed and direction changes significantly between the top of the mast and sea level, due to the apparent wind vector being formed by subtracting the yacht velocity off the true wind velocity, and their differences vary considerably between the foot and head of a sail.

Both forces and pressures can be measured onboard. As mentioned above, measuring the pressure distributions is preferable to measuring forces, as it gives a much more complete description of the loading process. It is more difficult to measure pressure measurements in downwind conditions than in upwind sailing conditions because the Apparent Wind Speed (AWS) is lower in the former case. The differential pressure across sails is of the order of magnitude of the dynamic pressure, which is, for instance, about 5.5 Pa for a 3 m/s AWS. To measure a pressure distribution along a sail section, pressure variations smaller than about 1 Pa should be measured. However, in one minute, the wind typically oscillates by about ±0.5 m/s, which leads to dynamic pressure oscillations of about ±2 Pa. Moreover, pressures can change by several Pascals per minute due to the incoming atmospheric turbulence.

Therefore on-water pressure measurements automatically take into account these dynamic effects, which are neglected or poorly modelled by numerical modelling and wind tunnel experiments, but on the other hand, the complexity of the real system makes the measurements quite complicated and, thus, less accurate.

2. The State of the Art of Pressure Measurements on Sails

Sail aerodynamics has been widely investigated with numerical modelling. From the 1960s to the end of the last century, most of the computations were performed using potential flow codes. In the past 10 years, RANS codes became very popular for studying downwind sails. A review of potential flow and RANS applications is presented in Viola, 2009. Over the past few years, only a few LES or DES applications on sails have been published (Wright et al., 2010; Braun & Imas, 2008) but the most important research institutes in sail aerodynamics are all investigating these techniques.

Viola & Flay, 2009, reviews wind tunnel force measurements on downwind sails, while Viola & Flay, 2010, reviews pressure measurements on sails performed on-the-water and in a wind tunnel. In the following paragraphs, a complementary review of force and pressure full-scale experiments on sails is provided.

Force measurements have been performed more rarely in full-scale than in wind tunnels, due to the difficulty and cost. Milgram et al, 1993, at the Massachusetts Institute of Technology (MIT), introduced the innovative concept of an instrumented framework structure located inside the 35-foot yacht *Amphetrete*. The frame connected the rigging to the hull and was instrumented with a 6-component balance that measured the aerodynamic forces in equilibrium with the hydrodynamic forces. Masuyama & Fukasawa, 1997, at the Kanazawa Institute of Technology, developed a similar concept on the yacht *Fujin*. These two papers are mainly oriented towards investigating the aerodynamics of yachts. Conversely, the research described by Hochkirch and Brandt, 1999, at the Berlin University was mainly focused on the hydrodynamics of yachts. They applied a similar "framework structure" concept to the 33-

foot yacht *Dyna*, as well as having an additional anemometer, and were able to measure the hydrodynamic forces on the yacht appendages.

Full-scale pressure measurements were performed for the first time by Warner and Ober, 1925, at the Massachusetts Institute of Technology (the tests were performed between 1915 and 1921). The authors used U-tube pressure manometers on the S-class yacht *Papoose*. Much later, Flay and Miller, 2006, reported the lessons learned by the Yacht Research Unit (YRU) of the University of Auckland in measuring pressures on the sails of the Farr1020-class yacht *Shokran*. The first pressure distribution with a large number of pressure taps (25 per side) was presented the same year by Puddu et al., 2006, from the University of Cagliari, Sardinia. The authors measured the pressures on the mainsail of a Tornado-class catamaran. Graves et al., 2008, measured the pressures on the mainsail of a IACC-class yacht, but only 5 pressure taps were used. The first modern pressure measurements (after Warner and Ober in 1925) on head sails was recently performed by Viola & Flay, in press. The authors measured pressure distributions on the mainsail and the genoa of the 24-foot yacht *Aurelie,* designed by Sparkman & Stephens.

As far as is known by the authors, pressure distribution on downwind sails have never been published. The present paper presents the first pressure measurements on an asymmetric spinnaker. The measurements were performed on a 1/3rd model-scale sail, which was designed for a 90-foot America's Cup class (AC33) yacht. The sail was tested on a 25-foot Platu25-class yacht.

3. Method

THE SAILS

In the late 2008s and early 2009s, it was not clear which yacht class would be used in the 34th America's Cup, and when and where the race would be held. Emirates Team New Zealand, the winner of the previous Louis Vuitton Cup, was investigating the design of the most likely class for the next event. The YRU, which is Emirates Team New Zealand's Official Scientific Advisor, asked North Sails New Zealand to manufacture a 1/3rd scale AC33-class asymmetric spinnaker for on-water testing. The spinnaker was built with 4 horizontal panels, which were sewed together with an overlap of about 100 mm at each joint. The overlapped panels made 3 horizontal pockets where 21 pressure taps per pocket were located, and the pockets were used to contain the tubes. Figure 1 shows a schematic drawing of the pressure taps located along the three overlapping joints.

The pressure taps were very flat thin plastic cones with base and top surface diameters of 50 mm and 40 mm, respectively. The cone height was 5 mm. The pressure taps had a hole in the centre of the top surface which connected to a metal 2 mm diameter tube protruding out the side of the tap, as shown in Figure 2. PVC tubes connected to the pressure taps conveyed the pressures to the transducers located inside the yacht cabin. The tubes from all the pressure taps were threaded to the luff (leading edge of the sail) inside the horizontal pockets and then down to the tack (corner of luff and sail foot) inside an additional vertical pocket.

The pressure distributions were measured on the leeward side while sailing on starboard tack (wind coming from the right hand side of the yacht), and on the windward side when sailing on the port tack (wind coming from the left hand side of the yacht). No pressure measurements were performed on the mainsail. Future research should aim to measure the pressure on the two sails simultaneously. The mainsail used in the on-water tests was a standard Platu25-class mainsail.

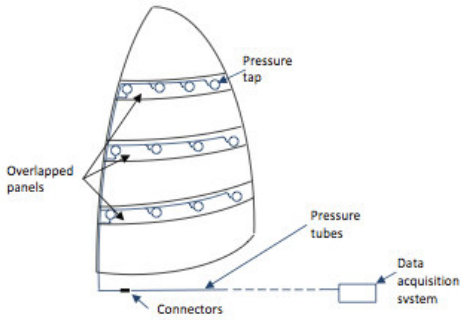

Figure 1: Schematic layout of the pressure-tapped sail (edited from Watier, 2010).

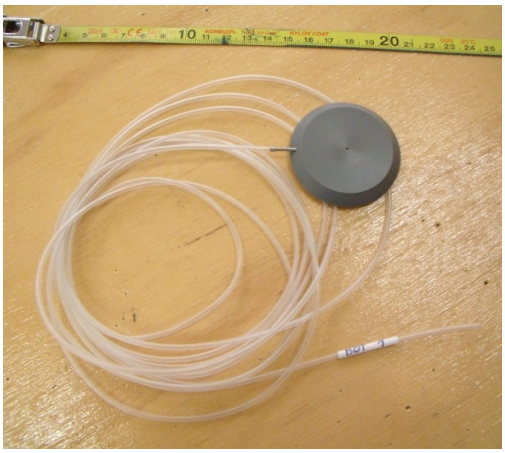

Figure 2: Pressure tap with pressure tube connected.

THE PRESSURE SYSTEM

The tubes were connected to the transducers, which were well protected inside the cabin. The pressure transducers had a range of ±450 Pa and a resolution of 9.25 mV/Pa with an accuracy better than ±0.5 Pa. Additional details describing the pressure system are provided by Fluck et al., in press. All the transducers were pneumatically connected to a reference static pressure tube. The tube was 10 m long and the end of the tube was located inside a porous box in a cabinet inside the cabin, which assured that the air inside the box had negligible velocity. The reference static pressure p_∞ was compared with the static pressures measured by Pitot-static probes fixed to a pole on the stern of the boat. The pole was about 2 m high and several Pitot-static probes were fixed onto it. The anemometers were deliberately pointed in different directions. All the static and the total pressures from the Pitot-static probes were connected to the transducers inside the cabin. When the boat was at the wharf, the pressure differences between p_∞ and the static pressures measured on the pole were found to be negligible, as expected. Conversely, the differences between the static pressures were larger while sailing. This was assumed to be due to the influence of the sails on the static pressures measured on the pole. For this reason, the reference static pressure p_∞ was taken to be that measured inside the cabin, and not by the probes on the pole.

Pressures were acquired at 100 Hz for 90 seconds. High frequency fluctuations would have been damped by the long tubes (up to 20 m long) and hence a higher sampling frequency would have resulted in additional and redundant stored data.

Pressures were measured using two different approaches. In the first case, pressures were measured with the yacht sailing in the most stable sailing state as possible, with the sails in a fixed state of trim and the yacht on a constant course. Pressures were recorded and averaged on the sampling period. In the second case, pressures were measured while one sail condition was changed at a constant rate. For instance, over 90 s the sail was trimmed in from fully eased to hard in. For these test cases the pressures were averaged in sets of about 15 s and the resulting 6 average values were used to show the pressure variation with the sail trim.

MEASURING THE DYNAMIC PRESSURE

The dynamic pressure was measured with the Pitot-static probes fixed onto the pole on the stern of the yacht. The pole was on the port side when pressures on the windward side of the sail were measured, and on the starboard side when pressures on the leeward side of the sail were measured. The pole was also inclined at about 20° from the vertical axis of the yacht, so

that the Pitot-static probes were always leaning to windward from the yacht. Figure 3 shows the pole supporting the probes while sailing upwind after the tests. It was found that the pressures measured by the Pitot-static probes on the pole were less affected by the sail trim, than when the pole was 2 m above the head of the mast.

Initially, a single pivoting Pitot-static probe was mounted on the pole. In a previous experiment (Viola & Flay, in press.), where pressures were measured on upwind sails, the wind was able to align the pivoting anemometer used with the wind direction. This setup was not appropriate for the present test, however, because the AWS was not high enough to align the anemometer into the wind. Therefore, three fixed Pitot-static probes aligned in different directions were used. The total-pressures from all three anemometers were measured at each acquisition. Then the pressure measured by the Pitot-static probe most aligned with the wind local wind direction was used as the reference dynamic pressure q_∞. In the present paper, q_∞ was between 4 and 40 Pa.

The AWA was measured with the standard on-board instrumentation located at the top of the mast.

4. Results and Discussion

Figure 4 shows the Platu25-class yacht sailing with the pressure-tapped asymmetric spinnaker. In the full-scale AC33-class yacht, the top of the spinnaker is at the same height as the top of the mainsail. Therefore, the measurements were performed with the mainsail lowered (one reef was taken) from the hoist shown in Figure 4, so that the heads of both sails lined up during the measurements. As a consequence, the lower centre of effort of the mainsail led to a lower heel angle of 10°, than that shown in Figure 4.

Three AWAs and several sail trims were measured. The full-scale asymmetric spinnaker was designed to be sailed at about AWA=80° in light air. The Platu25-class yacht does not have a very large transverse stability, and therefore an AWA of 80° resulted a fairly small angle to be sailed with a spinnaker. Two additional AWAs were tested, namely 120° and 170°.

The pressure signals were remarkable unsteady. In fact, it was not possible to keep a constant sail trim and to sail a constant course. When a gust arrived, the AWS increased and so did the heeling moment. The yacht began heeling and the helmsman reacted immediately to change the course to increase the AWA. The yacht then straightened up and accelerated due to the reduction in hydrodynamic resistance. The increased boat speed led to a lower AWA and the sail then had to be trimmed in. As soon as the gust passed by and the yacht slowed down, the sail became over-trimmed and it had to be eased. Therefore, the AWA and the sail trim were changing continuously. The frequency and the amplitude of the changes in the course and in the sail trim are certainly larger on small yachts, such as the Platu25 class, than on large yachts, such as the AC33 class, and thus much care has to be taken in transferring the results obtained on a tender keel boat to a more stable large keel boat with a relatively much heavier keel.

The dynamic movement of the sail led to vertical wrinkles, which were continually appearing and disappearing. The wrinkles were often in the same positions on the sail. Peaks and hollows in the averaged pressure distributions along horizontal sections in relation to these wrinkles are discussed later.

The pressure measurements are presented in terms of pressure coefficient *Cp*, defined as the difference between the pressures measured by the pressure taps on the sail and the reference static pressure p_∞, measured inside the cabin, divided by the reference dynamic pressure q_∞, measured by the selected Pitot-static probe on the pole. The pressure distributions presented have been smoothed to present general trends.

Figure 3: Pole supporting the Pitot-static probes (shown while sailing upwind after the tests).

Figure 4: The yacht and the pressure-tapped sail. The black bands show the locations of the pressure taps.

GENERAL PRESSURE DISTRIBUTION TRENDS

Pressure distributions on sails can be explained in terms of classical aerodynamic theory for thin airfoils. In a middle height section, the flow direction can be considered mainly in the chord-wise direction. If the local flow at the leading edge is tangent to the sail, then the angle of attack is named *ideal angle of attack*. In this case, the stagnation point is at the leading edge, where the pressure is nearly equal to the dynamic pressure and $Cp \approx 1$. On the leeward side, Cp decreases along the chord until about the maximum curvature of the sail, and then increases again until roughly $Cp \approx 0$ if there is no trailing edge separation, or until $Cp \approx -1$ if there is trailing edge separation. On the windward side, the flow is slow and Cp is nearly the stagnation pressure for most of the chord length. At the trailing edge, Cp decreases to match the leeward-side trailing-edge pressure.

If the flow at the leading edge presents a positive angle with the leading-edge sail profile, a leading-edge separation bubble occurs. At the leading edge, the flow separates on the leeward side of the sail and reattaches in the first quarter of the chord length. The pressure on the leeward side decreases abruptly near the leading edge, and then increases until roughly the reattachment point. Further downstream, the pressure decreases again due to the sail curvature and then increases after the maximum sail curvature. The pressure increase can lead to trailing edge separation. If separation occurs, the pressure recovery is interrupted and the pressure remains constant and equal to the so-called *base pressure*. Figure 5 shows a schematic drawing of the flow field and the correlated pressure distribution.

As far as the flow does not stall, the higher the angle of attack, the higher is the suction near the leading edge. At high angle of attacks, the leading edge suction peak is much higher than the cambered-related suction peak and, thus, the second is not visible. When the flow stall and the flow does not re-attach downstream, the leading edge suction peak decreases. At very

high angle of attacks, higher than the stall angle, the pressure becomes almost constant and equal to the base pressure.

The stall angle on the mid section of an asymmetric spinnaker is above 20°. On an equal two-dimensional section, the stall angle would have been significantly lower. On three-dimensional sails, the tip vortices take a large amount of flow from the windward side to the leeward side, increasing the pressure on the leeward side. Therefore, the flow is able to reattach downstream at high angle of attacks. More details about the pressure distribution on downwind sails can be found on Viola & Flay 2009 and 2010.

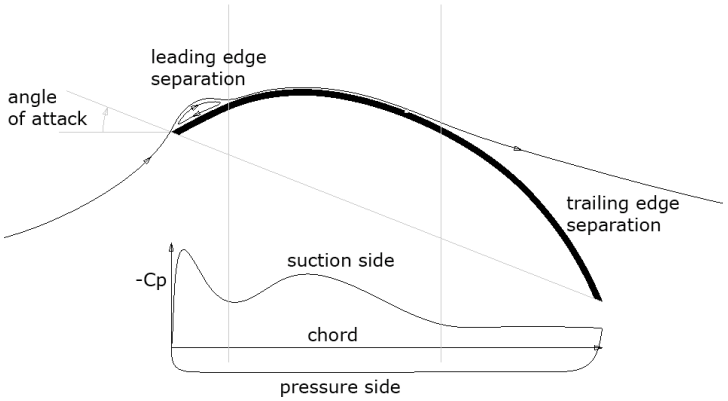

Figure 5: Schematic drawing of the flow field and of the correlated pressure distribution.

PRESSURE DISTRIBUTIONS FOR DIFFERENT TRIMS

Figure 6 shows *Cps* on the leeward side of the 3 horizontal sections of the asymmetric spinnaker. *Cps* are plotted along the curve length for each sail section and for 4 different sail trims. The sail is initially eased as much as possible (*max eased* trim in Figure 6). The low angle of attack on the top sections of the sail leads to flapping of the leading edge. The pressures on the top section ($3/4^{th}$ of the sail height) show that the sail is trimmed at the *ideal angle of attack*. On the lower sections, a leading edge suction peak occurs, and the *Cp* shows a suction peak within the first quarter of the sail. In the second half of the curve length, trailing edge separation occurs and the *Cp* becomes almost constant.

When the sail is trimmed in just enough to stop the luff from flapping (trim *eased* in Figure 6), a leading edge suction peak occurs on the top section. Sailors would generally consider this the optimum trim. On the middle and bottom sections, the suction peak decreases due to movement of the trailing edge separation point upstream along the curve length. On the top section near the trailing edge, *Cp* decreases up to -3. This pressure trend is unexpected and should be investigated further. It could be related to the interaction of the asymmetric spinnaker with the mainsail, or to a local stable vortex with a significant reverse velocity at the trailing edge. It should be noted that a similar trend has never been measured in wind-tunnel tests, as far as the authors are aware. On trimming further in, (from trim *tight* to *max tight* in Figure 6), stall occurs and the leading edge suction peak decreases. *Cp* becomes almost constant and is equal to -1.

On the windward side (Figure 7), *Cp* is almost independent of the sail trim and, therefore, *Cp* measured at the optimum trim only is shown. *Cp* is less than 1 at the trailing edge, which shows that at the stagnation point there is a significant span-wise velocity component. Along the chord length, *Cp* decreases only near the trailing edge, where it matches *Cp* on leeward side. Because the pressure tap closest to the trailing edge was about 100 mm from the trailing edge, the last measured *Cp* on the leeward side is not equal to the last measured *Cp* on the windward side.

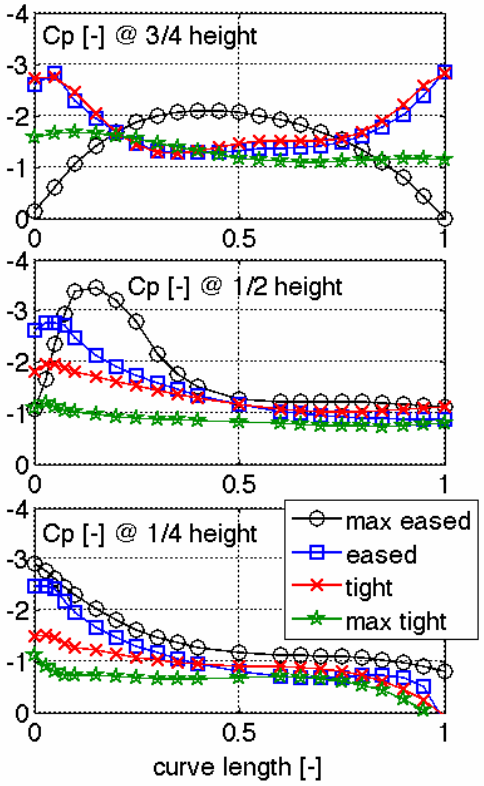

Figure 6: Leeward *Cp* on the 3 sail sections for 4 sail trims.

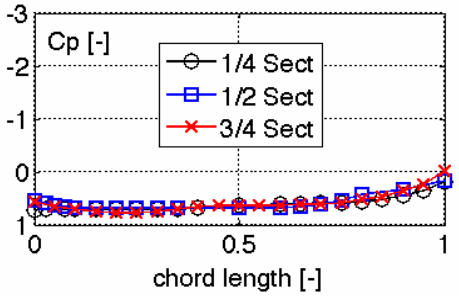

Figure 7: Windward *Cp* on the 3 sail sections.

PRESSURE DISTRIBUTIONS FOR DIFFERENT AWAS

Figure 8 shows *Cps* on the leeward side of the 3 horizontal sections of the asymmetric spinnaker. The sail was re-trimmed to the optimum trim at each AWA. On the top section, when sailing at AWA=120°, the *Cp* shows the unexplained and rather interesting trailing edge suction. It should be noted that the unexpected suction do not occur at AWA=80°, while in the previous test (Figure 4), when different trims were tested at AWA=80°, the unexpected suction occurred at the optimum trim.

Figure 8 shows that the sail can be trimmed at AWA=80° and AWA=120° to achieve a high suction on the entire leeward side of the sail. Conversely, when the AWA is increased further, the sail cannot be eased sufficiently and stall occurs. The integral of *Cp* along the curve length represents most of the aerodynamic force due to the sail. Figure 8 thus indicates that the aerodynamic force is decreased when stall occurs.

The *Cp* on the windward side is not presented here because it does not present any significant differences from the *Cp* trends shown in Figure 7.

FULL-SCALE AND WIND-TUNNEL COMPARISON

Figure 9 shows *Cps* on the leeward side of the 3 horizontal sections of the asymmetric spinnaker, measured on-the-water and in the wind tunnel respectively. *Cps* were measured on water for the optimum trim at AWA=80°. Wind-tunnel measurements were performed with a 1/15th model-scale flexible sail at the optimum trim at AWA=70°. A detailed description of the wind tunnel measurements can be found in Viola & Flay 2009 and Viola & Flay 2010. Figure 9 shows very good agreement and few differences between the *Cps* measured in full-scale and in the wind tunnel. The first difference is due to the unexplained trailing edge suction on the top section of the full-scale test, which has already been discussed. The second difference is the more positive pressure recovery related to the leading edge reattachment, which could be due to a tighter trim in the full-scale experiment. In fact, the higher the angle of attack, the higher the leading edge suction peak and the smoother the pressure recovery. A tighter trim is thought to have been used in the full-scale experiment due to trimming in the unstable conditions. Conversely, the stationary wind conditions and fixed yacht model attitude in the wind tunnel allowed a more eased trim to be used.

The different leading edge pressure distributions could also be due to a Reynolds number effect. The wind-tunnel tests were performed at Reynolds number about 1/10th lower than the full-scale Reynolds number. The higher Reynolds number in full-scale could affect the leading edge separation bubble and thus the leading edge pressure distribution. Finally, leading edge separation bubbles can be affected by different characteristics of wind turbulence. However, the authors consider that it is more likely that the differences are due to different sail trims, rather than to Reynolds number or to different wind turbulence characteristics.

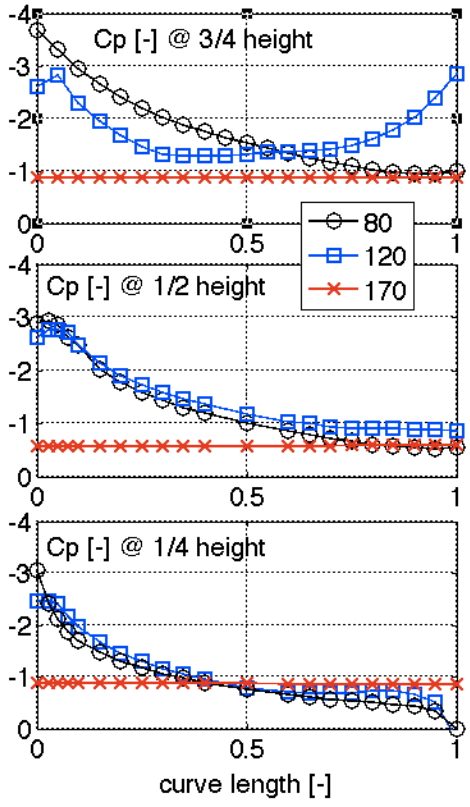

Figure 8: Leeward *Cp* on the 3 sail sections for 80°, 120° and 170° AWA.

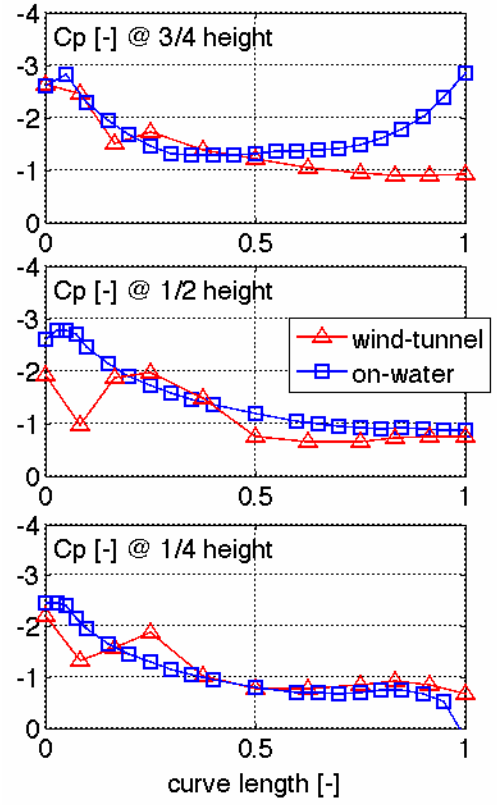

Figure 9: Wind-tunnel and on-water leeward *Cps* on the 3 sail sections.

5. Acknowledgments

The authors wish to acknowledge the support of staff and students in the Yacht Research Unit, and in particular, the authors are grateful to Mr. Baptiste Watier and Mr. Etienne Gauvain for the passion and the support in managing and performing the on-water and wind tunnel experiments. The authors also acknowledge the support of Dr Nick Velychko in building and supporting the multi-channel pressure system.

6. Conclusions

Pressure distributions on sails have been measured only rarely. In particular, on-water pressure measurements have been performed only in upwind sailing conditions. As far as known by the authors, the present paper presents the first pressure measurements on sails flown in downwind sailing conditions. While numerical modelling and wind tunnel experiments neglect or model relatively poorly the unsteadiness of the wind, the movement of the sails and the yacht, on-water sail tests automatically take them into account.

Pressures were measured using 63 pressure taps distributed along three horizontal sections at 1/4th, 1/2nd and 3/4th of the sail height, respectively, on an asymmetric spinnaker. The sail was designed for Emirates Team New Zealand, a possible challenger for the 34th America's Cup, when it was expected to be sailed with AC33-class yachts. Pressure distributions were measured for several sail trims and 3 apparent wind angles (AWAs) on both the leeward and windward sides of the sail.

The main conclusions that can be drawn from the experiments are summarised below.

PRESSURE DISTRIBUTIONS FOR DIFFERENT TRIMS

- For the optimum sail trims, the *Cp* on the leeward side of the sail near the leading edge has a suction peak between *Cp* = -3 and *Cp* = -4, and downstream, *Cp* increases monotonically.
- On the leeward side, *Cp* is almost constant and is slightly less than 1. *Cp* decreases near the trailing edge to match the leeward-side trailing-edge suction.
- In some conditions, which were not well defined, on the top section only, an unexplained suction was measured near the trailing edge.
- Trimming-in the sail caused the leading edge suction to decrease due to trailing edge separation, until *Cp* becomes almost constant and equal to – 1 when stall occurs.

PRESSURE DISTRIBUTIONS FOR DIFFERENT AWAS

- Almost the same pressure distribution is achieved by re-trimming the sail for AWA=80° and AWA=120°. Conversely, at higher AWAs it was not possible to ease the sail enough and stall occurred. Therefore, *Cp* is almost constant and equal to – 1.
- On the leeward side, *Cp* is almost constant between 0 and 1, and it decreases near the trailing edge to match the leeward-side trailing-edge suction.

FULL-SCALE AND WIND-TUNNEL COMPARISON

- Full-scale and wind tunnel pressure measurements showed very good agreement and few differences on the leeward pressure distributions.
- The unexpected suction on the top section near the trailing edge has never been reported from wind tunnel test results.
- The pressure recovery is related to leading edge reattachment, which occurs around the first quarter of the curve length, and was visible in the wind tunnel-measurements but not in the full-scale measurements. Several possible reasons for this have been discussed.

7. References

Braun J.B. & Imas L., 2008. High Fidelity CFD Simulations in Racing Yacht Aerodynamic Analysis, *in the proceedings of The 3rd High Performance Sailing Yacht Conference (HPYDC3)*, 2nd-4th December, pp. 168-175, Auckland, New Zealand.

Flay R.G.J. & Millar S., 2006. Experimental Consideration Concerning Measurements in Sails: Wind Tunnel and Full Scale, *in the proceedings of The 2nd High Performance Yacht Design Conference (HPYDC2)*, February 14th-16th, Auckland, New Zealand.

Fluck M., Gerhardt F.C., Pilate J. and Flay R.G.J., in press. Comparison of Potential Flow Based and Measured Pressure Distributions Over Upwind Sails, *Journal of Aircraft*.

Gaves W., Barbera T., Broun J.B., Imas L. 2008. Measurements and Simulation of Pressure Distribution on Full Size Scales, *in the proceeding of The 3rd High Performance Yacht Design Conference (HPYDC3)*, December 2nd-4th, Auckland, New Zealand.

Hochkirch K. & Brandt H., 1999. Full-Scale Hydrodynamic Force Measurement on the Berlin Sailing Dynamometer, *in the proceedings of The 14th Chesapeake Sailing Yacht Symposium (14CSYS), SNAME,* pp. 33-44, 30th January, Annapolis, USA.

Masuyama Y. & Fukasawa T., 1997. Full-Scale Measurements of Sail force and Validation of Numerical Calculation Method, *in the proceedings of The 13th Chesapeake Sailing Yacht Symposium (13CSYS), SNAME*, pp. 23-36, 25th January, Annapolis, USA.

Milgram J.H., Peters D.B., Eckhouse D.N., 1993. Modeling IACC Sail Forces by Combining Measurements with CFD, *in the proceedings of The 11th Chesapeake Sailing Yacht Symposium (11CSYS), SNAME*, pp. 65-73, 29th-30th January, Annapolis, USA.

Puddu P., Erriu N., Nurzia F., Pistidda A., Mura A., 2006. Full Scale Investigation of One-Design Class Catamaran Sails, *in the proceeding of The 2nd High Performance Yacht Design Conference (HPYDC2),* February 14th-16th, Auckland, New Zealand.

Viola I.M., 2009. Downwind Sail Aerodynamics: a CFD Investigation with High Grid Resolution, *Ocean Engineering, vol. 36, issues 12-13,* pp. 974-984.

Viola I.M. & Flay R.G.J., 2009. Force and Pressure Investigation of Modern Asymmetric Spinnakers, *International Journal of Small Craft Technology, Trans. RINA*, vol. 151, part B2, pp. 31-40, 2009, DOI: 10.3940/rina.ijsct.2009.b2.98. Discussion in *Trans. RINA*, vol. 152, part B1, pp. 51-53.

Viola I.M. & Flay R.G.J., 2010. Pressure Distribution on Modern Asymmetric Spinnakers, *International Journal of Small Craft Technology, RINA,* Vol. 152, part B1, pp. 41-50.

Viola I.M. & Flay R.G.J., in press. Full-scale Pressure Measurements on a Sparkman & Stephens 24-foot Sailing Yacht, *Journal of Wind Engineering and Industrial Aerodynamics,* DOI:10.1016/j.jweia.2010.07.004

Viola I.M., Pilate J., Flay R.G.J., submitted. Upwind Sail Aerodynamics: a Pressure Distribution Database for the Validation of Numerical Codes, *International Journal of Small Craft Technology.*

Viola I.M. & Ponzini R., 2009. Sailing Past a Billion, *Ansys Advantage*, vol. 3, issue 2, pp. 47-48.

Warner E.P. & Ober S., 1925. The aerodynamics of Yacht Sails, *in the proceedings of The 3rd General Meeting of the Society of Naval Architects and Marine Engineers,* 12th-13th November, New York, USA.

Watier P.B., 2010. Comparison of Full-Scale and Model-Scale Measurements of the Aerodynamics of an Asymmetric Spinnaker, *MEng Thesis, DTU Mechanical Engineering, Technical University of Denmark*.

Wright A., Claughton A., Paton J., Lewis R., 2010. Offwind Sail Performance, Prediction and Optimisation, *in the proceedings of The 2nd International Conference on Innovation in High Performance Sailing Yachts (INNOV'SAIL)*, 30th June – 1st July, Lorient, France.